Article

Research and Experiment on Airflow Field Control Technology of Harvester Cleaning System Based on Load Distribution

Duanxin Li, Qinghao He, Dong Yue, Duanyang Geng *, Jianning Yin, Pengxuan Guan and Zehao Zha

College of Agricultural Engineering and Food Science, Shandong University of Technology, Zibo 255200, China; 22503060013@stumail.sdut.edu.cn (D.L.); 22503060002@stumail.sdut.edu.cn (Q.H.); 22503060004@stumail.sdut.edu.cn (D.Y.); 23503060450@stumail.sdut.edu.cn (J.Y.); 23403010296@stumail.sdut.edu.cn (P.G.); 23503060436@stumail.sdut.edu.cn (Z.Z.)
* Correspondence: dygxt@sdut.edu.cn

Abstract: The wind sieve cleaner is widely used in the screening system of combine harvesters due to its compact structure and efficient screening capability. In order to study more deeply the feeding load distribution of the combine harvester and the influence of the airflow field on the clearing effect, a mechanical analysis method was adopted to analyze the dynamics of the material in the inclined airflow, and a kinetic model was established. At the same time, the motion state of the material in the airflow field was explored, and combined with the actual orthogonal test, the response surface model of factors and indicators was established. Experimental validation was carried out. It provides an important research foundation and theoretical basis for optimizing the structural parameters of the screening system and improving its operational performance.

Keywords: air sieve type cleaning device; combine harvester; test parameter optimization

1. Introduction

The cleaning device is an important part of the grain harvester [1–3]. Its working performance has a great influence on the cleaning effect and loss of the harvester. Especially in the operation process of the harvester, when the parameters such as crop yield, operation speed, maturity, and moisture content change, it is often necessary to adjust and control the parameters such as the airflow speed and direction of the cleaning system and the opening degree of the fish scale sieve in time to meet the operation requirements of the cleaning system under the current conditions when the load on the sieve changes [4–7]. In order to improve the cleaning effect of the harvester and improve the adaptability of the operating parameters of the cleaning system to the load change, a large amount of research has been carried out on it. In order to explore the motion state of flax in the cleaning room, Zhao et al. established a gas–solid coupling simulation model of flax threshing to simulate the behavior of flax threshing materials in a dual-channel gas sieve separator. The CFD-DEM coupling method was used to simulate the motion process of flax in the separation device, and the distribution characteristics of the airflow vector were revealed. By analyzing the migration path and distribution state of the material in the vibrating screen, the change trend of the movement trajectory and migration speed of the components of the flax threshing material in different regions with time were revealed [8]. In order to explore the movement state of oats in the cleaning room, Li et al. used particle image velocimetry (PIV) technology to study the airflow velocity field of the cleaning machine. The measured airflow velocity field space was divided into nine longitudinal planes, and the movement of oats in the cleaning room was recorded by a high-speed digital camera. The results show that the transverse distribution of airflow velocity field in each longitudinal section is not uniform, oats and impurities move along the direction of airflow reflux, and the transverse flow in the radial direction above the middle sieve is irregular [9]. Geng et al. of Shandong University of Technology conducted an experimental study on the influence of the working parameters

of the centrifugal fan on the airflow field in the clean room. The Fluent simulation software 2021R1 was used to conduct a single factor test on the influence of the air supply distance, fan speed, and blade number of the centrifugal fan on the airflow velocity of the screen surface. The variation law of the airflow velocity before, during, and after the screen, and the relationship between the deviation degree of the airflow after the screen and the related parameters were explored [10]. In order to explore the relationship between cleaning load and airflow velocity, Li et al. of Jiangsu University designed a cleaning system based on a multi-channel fan. According to the research, the increase in cleaning load leads to the decrease in air velocity in the fan and air duct. The experiment shows that the air flow recovery speed at the outlet of the fan and in the tail screen is the key to affect grain loss. The decrease in airflow velocity in the 300~540 mm area of the cleaning section significantly affected the grain impurity rate [11]. In order to solve the problem of excessive cleaning losses during harvester operation, Xu et al. developed a multi-channel cleaning device performance monitoring system. The grain loss rate and impurity rate were reduced by adjusting the fan speed, deflector angle, and sieve opening. When the grain loss rate is high, the wind speed is reduced to minimize grain loss, and when the grain loss is stabilized, the fan speed is increased to improve cleaning efficiency [12].

In summary, regulating the airflow field distribution in the cleaning room is the key to improving the operational performance of the air-screen combined cleaning system. Although previous research has focused on improving the distribution of screened material, optimizing fan structure, and working parameters, it has not yet been based on changes in the screened material load in the context of airflow field distribution research. Therefore, in this study, the dynamic analysis of the material in the inclined airflow of the cleaning fan was carried out by means of mechanical analysis. The change process of cleaning when the screening load changed was studied, and the influence of fan speed, feeding amount, and guide plate on the cleaning process was discussed. It is important to carry out this study to reduce cleaning losses and improve the quality of the cleaning process.

2. Materials and Methods

2.1. Structure and Working Principle of Harvester Cleaning Device

The screening system of a grain combine harvester mainly consists of a fan, jitter uniform distribution plate, upper sieve, lower sieve, tail sieve, corn conveyor, impurities conveyor, and so on, and its structure is shown in Figure 1.
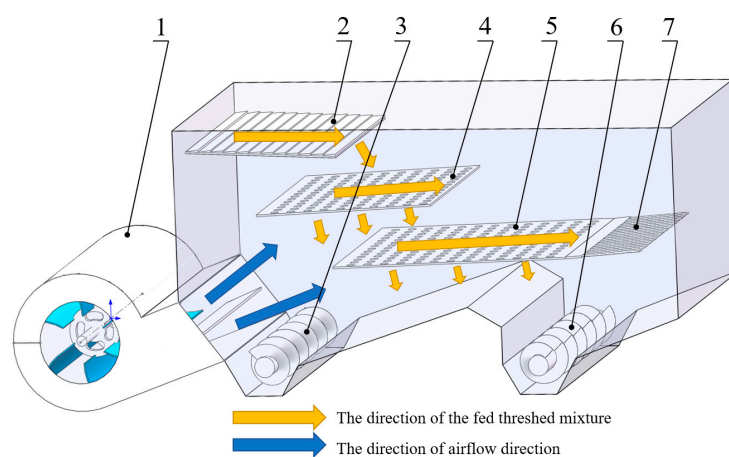
Figure 1. Schematic diagram of the structure of the cleaning system. (1). Fan. (2). Jitter uniform distribution plate. (3). Corn conveyor. (4). Upper sieve. (5). Lower sieve. (6). Impurities conveyor. (7). Tail sieve.

During harvester operation, the sieve through the shaking plate reciprocating vibration causes material longitudinal and transverse uniform distribution and upward sieve transport, the upper and lower sieves form a sieve box and do reciprocating motion, so

that the grains are separated from the material and long impurities, with light impurities in the sieve box, and by means of the airflow are transported backward and discharged out of the machine [13,14]. During this process, the threshing drum and separation concave plate work together to remove the grains. Subsequently, the extracted material is continuously transported backward under the sieve's action, during which some grains are separated through the sieve. Consequently, the load on the sieve surface inevitably transitions from heavy to light along its length, which determines the transport of impurities by means of the air velocity; they must also appear at the front of the high speed and at the back of the distribution of a slightly lower distribution law, especially in the front of the upper sieve. Due to the high content of corn in the mixtures, the air flow must pass through the screen surface, and the mixtures must show a fluidized state in order to achieve the separation of impurities and grains, so this position requires the air velocity of the screen box to be such that the impurities are separated from grains. Therefore, the airflow speed in this position is required to be higher, while the rear part almost always has light impurities, large impurities, and heavy impurities, of which the light impurities are discharged with the airflow, while the large and heavy impurities can only be discharged out of the machine by means of the reciprocating motion of the sieve box [15].

In this process, in addition to the role of the vibrating screen, the size and distribution of the airflow speed on the sieve appear to be very important for impurities in the cleanup. If the speed of the airflow is too small or the distribution is unreasonable, it will lead to an increase in the impurity rate of the corn or an increase in the loss during the cleanup process. Therefore, reasonable control of the airflow speed and distribution in the harvester is of great significance to improving the cleanup system of the harvester [16].

The grain harvester cleaning process removes the material in the vibrating screen and uses the of airflow to blow light impurities away from the screen surface, and under the action of the airflow field gradually backward, so that they are discharged from the machine, and the grains are moved along the sieve to the back by a continuous process of throwing through the sieve holes, to achieve the separation of the grains and impurities. Due to the sieving out of the material in the static state, light impurities are difficult to separate from the material above the sieve wrapped in the material, so it is necessary to increase the air velocity to achieve sieving from the static state to the fluidized stat. In general, the airflow velocity needs to be no more than the suspension velocity of the grains at the highest, an no less than the critical wind speed of the light debris blowing out at the lowest.

2.2. The Requirements of the Cleaning Process on the Airflow Field

From the point of view of the loss rate, the position of the grain landing on the screen surface should be as close as possible to the initial position in the length direction of the screen surface, in order to make full use of the effective working length of the sieve, and to reduce the increase in the entrainment loss of the corn; the position of the impurity landing point should be as far as possible from the feeding position, in order to reduce the impurity obstruction of the sieve holes, and to increase the ability of the corn to pass. For light impurities and so on, a one-time blowing directly out of the cleaning chamber outside is required, so that is they are no longer mixed with the grains on the screen surface; for larger impurities, they should be blown to the end of the screen to reduce seed accumulation to reduce the clearing burden of the vibrating screen.

From the perspective of cleaning efficiency, most of the grains in the threshing drum are removed before reaching the screen. This results in a concentration of grains and impurities mixed together at the front of the screen. Therefore, a higher wind speed and increased air volume are required to disperse the dislodged mixtures. The air volume is used to blow the mixtures through the grains and out through the upper sieve, while at the same time, most of the lighter impurities are blown towards the rear of the machine. If there is no airflow or insufficient airflow through the front part of the upper sieve, it will not be possible to disperse the mixtures, making it difficult to separate the grains from them. This

will lead to the accumulation of a large quantity of mixed material on the surface of the sieve in severe cases. As the materials continue to move towards the rear of the sieve, due to the continuous penetration of grains through the sieve, the proportion of light debris on the sieve gradually increases. To reduce the loss of grains at the rear of the sieve surface, the airflow speed at the rear should be reduced compared to the airflow speed at the front. The required airflow velocity is also influenced by factors such as the state of the threshed mixture being fed, the thickness of the threshed mixture layer, and other factors [17].

The forces on the grains or light impurities in the air flow field are analyzed as shown in Figure 2. The grains and light impurities are subjected to gravity G_1, aerodynamic force F_1, and buoyancy F_2 in the air flow field.
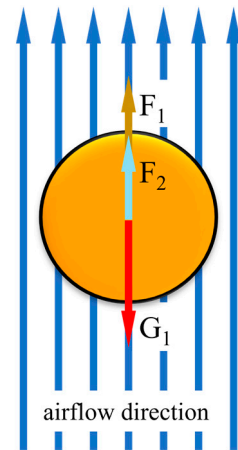
Figure 2. Force analysis of materials in an air flow field.

Where the F_1 and F_2 are:

$$\begin{cases} F_1 = \frac{1}{2}C\rho_1 Sv^2 \\ F_2 = \rho_1 gV \\ G_1 = m_1 g \end{cases} \tag{1}$$

Based on the above equation, in order for the threshed mixture to be fluidized, the force of materials in an air flow field can be expressed as:

$$\frac{1}{2}C\rho_1 Sv^2 + \rho_1 gV = m_1 g \tag{2}$$

Among them, the influence of buoyancy is small and negligible.

$$v = \sqrt{\frac{m_1 g}{k\rho_1 A}} \tag{3}$$

where G_1 = gravity of grain or light debris, N; F_1 = aerodynamic force of the grains or light impurities, N; F_2 = buoyancy of the grains or light impurities, N; C = coefficient of air resistance; ρ_1 = density of air, kg/m^3; S = windward area of grain or light sundries, m^2; V = volume of grain or light sundries, m^3; v = the relative velocity of grain or light sundries in the vertical direction in the airflow field., m/s; V_P = suspension velocity of grain, m/s; V_K = floating speed of grain, m/s.

When $V > V_P$, light debris will be blown off the screen surface to achieve the separation of light debris and grain. However, when the airflow velocity is too large, that is, when $V > V_K$, it will cause grain to leave the cleaning room, thus losing the opportunity to cross the sieve hole, resulting in an increase in cleaning loss. On the contrary, when $V \leq V_P$, at that time, the light impurities mix with the grain and it is difficult to break away from the sieve surface, which reduces the probability of the grain passing through the sieve hole. This not only leads to an increase in the impurity rate of the grain, but also causes the sieve

to be blocked by the impurities, and the cleaning loss would also increase. Therefore, the airflow velocity v should satisfy $V_P < V < V_K$.

As mentioned above, the light impurities in the screened material must be transferred from the material above the sieve to the surface of the sieve first, and then can be separated from the screened material under the action of the airflow. So, in order to ensure the realization of this process, the conditions for the screened material to be detached from the screen surface under the action of the airflow are investigated [18].

In order to simplify the analysis process and explore the influence law of airflow on the quality of clearing, it is assumed:

1. In order to determine the effect of airflow on the movement of the screened material, the vibration effect of the lower sieve on the movement pattern and distribution structure of the screened material is ignored;
2. Given that the screened material is uniformly dispersed from the shaking deflector plate to the upper sieve, it is approximated that the screened material possesses a homogeneous, equal-thickness, and uniformly distributed structure;
3. Prior to the removal of the sieve load from the sieve, the sieve load is considered a stable, impermeable, and homogeneous structure. It is assumed that the cleaning chamber is sealed and there is no airflow leakage;
4. The flow path of the airflow through the sieve is irregular and non-uniform, but the fluid's distribution structure is approximately consistent across any cross-section.
5. Since the width and length of the screen surface significantly exceed the thickness of the screened material, the pressure drop effect in the material thickness direction due to the screen's dimensions is not considered in the analysis.

When the air flows at a lower speed through the screen onto the material layer, the porosity of the material layer remains basically unchanged. Grains and light impurities, due to air resistance, are less affected by their gravity, so grains and light impurities remain stationary. With the increase in air velocity, the material layer of grains and impurities tends to become loose, and the material layer volume expands. When the air velocity continues to increase to a certain value, the material layer between the particles becomes fluffy and begins to tend towards a fluidized state. When it reaches the fluidized state, the pressure drop no longer increases with the increase in air velocity. The state before it reaches the fluidized state is analyzed.

Where Δp = pressure drop of the threshed mixture, Pa; ε = porosity of the threshed mixture, %; μ = dynamic viscosity of air, Pa s; ρ = air flow density, kg/m²; d_a = equivalent diameter of the threshed mixture, m; u = air flow velocity in the vertical direction, m/s; L = thickness of the threshed mixture, m; the pressure drop of the airflow through the sieve can be obtained by the Eugen formula (non-spherical particles):

$$\frac{\Delta p}{H} = 150\frac{(1-\varepsilon)^2}{\varepsilon^3}\frac{\mu u}{d_a^2} + 1.75\frac{(1-\varepsilon)}{\varepsilon^3}\frac{\rho u^2}{d_a} \tag{4}$$

According to the Eugen formula, the first term on the right side of the formula is the viscous loss of the airflow through the screen upper material, the second term is the inertia loss, the dislodged material is larger particles, the screen upper material is in the fluidized state, the Reynolds number is greater than 1000; in the case of a larger Reynolds number, the inertial loss is dominant, and the effect of viscous loss on the pressure drop can be neglected [18–21]. Considering only the inertia loss, the above equation can be expressed as:

$$\frac{\Delta p}{H} \approx 1.75\frac{(1-\varepsilon)}{\varepsilon^3}\frac{\rho u^2}{d_a} \tag{5}$$

Based on the above formula, the pressure drop of the threshed mixture can be expressed as:

$$\Delta p \approx 1.75\frac{(1-\varepsilon)}{\varepsilon^3}\frac{\rho u^2 H}{d_a} \tag{6}$$

Obviously, the air pressure drop across the sieve varies according to porosity, material density, air velocity, material layer thickness, and particle equivalent diameter; for an equal speed operation process (where the feed amount is unchanged), the pressure drops with the thickness of the layer, the initial velocity of the airflow, etc., and with the increase in the thickness of the material layer, the upper and lower surfaces of the screen on the upper and lower surface of the air pressure drop is greater; conversely, the pressure drop is smaller on the upper and lower surfaces of the screen. Eventually, when the airflow velocity through the screened material increases to the floating velocity of the screened material, the material is in the fluidized state. At this time the bed pressure drop is equal to the net weight of the material layer, and no longer increases with the increase in airflow.

When the material layer reaches the critical fluidization state, in the sieving chamber, the action of the airflow on the screened material in the closed sieving chamber can be approximated and abstracted. With the increase in the airflow pressure, when the airflow pressure drop is equal to the weight of the screened material (mg), the screened material tends to fluidize; that is, the screened material has a tendency to leave the screen surface. For the force analysis of the screened material, in this state, there are:

F_3 = force of air flow on the threshed mixture on sieve, N; F_4 = the buoyancy of the threshed mixture, N; G_2 = the gravity of the threshed mixture, N; ΔP = the pressure difference of the airflow on both sides of the sieve surface, Pa; ρ_2 = density of gas, kg/m^3; ρ_3 = density of the threshed mixture, kg/m^3; L = the thickness of the threshed mixture, m; A = the cross-sectional area facing the airflow, m^2; ε = the porosity of the threshed mixture, %; V = volume of the threshed mixture, m^3. The force on the threshed mixture on sieve is shown in Figure 3.

$$\begin{cases} F_3 = \Delta P \cdot A \\ F_4 = \rho_2 g V_p = \rho_2 g \cdot A H_1 (1 - \varepsilon) \\ G_2 = \rho_3 g V_p = \rho_3 g \cdot A H_1 (1 - \varepsilon) \end{cases} \tag{7}$$
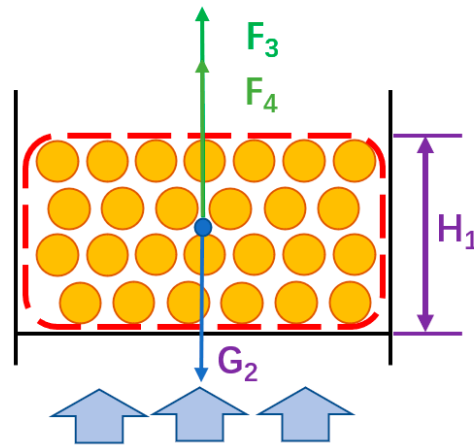

Figure 3. Force analysis of a material layer in a gas flow field.

When the threshed mixture reaches the critical fluidization state, we have:

$$\Delta P_1 \cdot A + F_4 = G_2 \tag{8}$$

Obviously, when the force is less than the gravity of the screened material, the screened material is in a stable stacking state; when the force is equal to the gravity of the screened material, the screened material reaches the critical tendency to leave the screen surface, and at this time, the material layer is in a fluidized state, and its pressure drop is:

$$\Delta P_1 = g H_1 (\rho_3 - \rho_2)(1 - \varepsilon) \tag{9}$$

From the above equation, it can be seen that when the screened material is in the fluidized state, the pressure drop of the airflow is related to the porosity of the screened material, the thickness of the material layer, and the density of the screened material; and it increases with the increase in these factors. That is, for the sieve to determine the component and the feeding amount, a certain pressure drop is required to maintain its fluidized state. However, as the porosity of the screened material, the thickness of the material layer, and the density of the screened material increase, the pressure drop will also increase. If this pressure drop exceeds the dynamic pressure provided by the cleaning device, it will lead to the transition of the sieve from the fluidized state to the static state, resulting in an increase in the impurity rate of the grains. Conversely, if these factors decrease, the pressure drop will decrease accordingly.

On the contrary, with the decrease in sieve porosity, the reduction in material layer thickness, and the increase in the equivalent diameter of the screened material, the pressure drop decreases, which will lead to the sieve remaining in the "boiling" state, thus increasing the cleaning loss. The larger the porosity of the sieve, the smaller the airflow blockage, which is consistent with the clearing operation process using a vibrating screen to enhance the sieve's effectiveness. That is, for a given grain combine harvester, as the amount of feed (including yield, moisture content, etc.) increases, the airflow rate must be adjusted accordingly to meet the needs of the sieve's operation. With a larger equivalent diameter of the screened material and a higher porosity of the sieve, the airflow rate can be appropriately reduced; conversely, the airflow rate needs to be increased.

In the process of cleaning, the airflow moves along the outlet into the cleaning room; the boundary of the cleaning room has no restriction on its role, and the change rule of its speed along the longitudinal direction of the cleaning room is similar to the change rule of the speed of the main section of the turbulent jet along the direction of the range. According to the principle of conservation of momentum, air velocity in any cross-section of the momentum flux is equal [22]. Then, we have:

$$\frac{V_s}{V_0} = \frac{0.492}{\sqrt{\frac{as}{b_0} + 0.41}} \tag{10}$$

Based on the above formula, the pressure drop of the threshed mixture can be expressed as:

$$V_s = \frac{0.492}{\sqrt{\frac{as_1}{b_0 \cos \alpha} + 0.41}} V_0 \tag{11}$$

where V_0 = air flow velocity of the cross section at the air outlet, m/s; a = coefficient of turbulence (when the outlet is a stable exhaust nozzle, it is 0.108); α = the angle between the bottom surface of the fan outlet and the horizontal plane, °; S = the distance traveled along the path from the position to the fan outlet, m; b_0 = width of the fan outlet, m; S_1 = horizontal distance from the fan outlet.

The velocity decomposition is shown in Figure 4. It can be seen from the formula that with the increase in the distance along the path, the airflow generated by the fan continuously exchanges energy and momentum with the static medium, driving the flow of the surrounding medium, resulting in the continuous attenuation of the airflow velocity. The lower airflow velocity will make it difficult to discharge the light debris in the rear of the screen surface. Therefore, by reducing the angle of the guide plate, the wind speed at the tail of the sieve can be slightly increased, which is conducive to the removal of impurities from the machine.
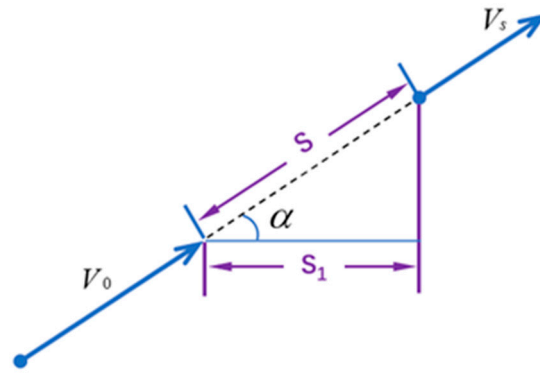
Figure 4. Orthogonal decomposition of velocity along the airflow velocity direction.

In the process of falling, the grain is approximately horizontally thrown under the action of air flow. where L = screening surface length, m; L_1 = the distance from the threshing position to the front end of the screen, m; h = the height distance from the screen surface, m; t_1 = time elapsed for grain to fall to sieve surface, s; β = the angle between the airflow direction and the horizontal plane, °. The grain motion state is shown in Figure 5.
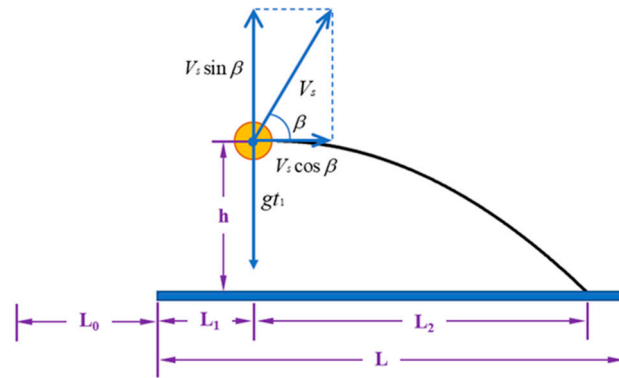

Figure 5. Velocity Decomposition of Grains in Vertical Plane of Cleaning Room.

The displacement along the vertical direction of the cleaning room can be expressed as:

$$h = -\frac{0.492}{\sqrt{\frac{as_1}{b_0 \cos \alpha} + 0.41}} V_0 \sin \beta t_1 + \frac{1}{2} g t_1^2 \tag{12}$$

The displacement along the length direction of the cleaning chamber can be expressed as:

$$L_2 = \int_0^{t_1} \frac{0.492}{\sqrt{\frac{as_1}{b_0 \cos \alpha} + 0.41}} V_0 t \cos \beta \, dt \tag{13}$$

In order to ensure that the corn is not blown out of the cleaning room due to the action of air flow, the displacement in the horizontal direction should satisfy $L_2 < L - L_1$. For the same type of machine, the distance between the threshing cylinder and sieve surface is known, and the maximum wind speed of the fan outside the cleaning room can be obtained through transformation.

2.3. Simulation Test of Harvester Cleaning Device

Gas sieve combination cleaning technology is one of the core technologies of grain combine harvesters [23,24]. Due to the quality of grain cleaning by the proportion of components, component density, component distribution uniformity, and other impacts, unreasonable job parameters will inevitably lead to grain harvester operation process cleaning loss or corn impurity rate increasing significantly.

In view of the large impact of airflow on the cleaning of the mixture, with reference to the common parameters of combine harvesters, combined with the preliminary pre-study [25], we set the fan outlet wind speed to 10.0 m/s, the deflector plate direction angle to 32° and 24°, respectively, with the help of ANSYS Fluent software 2021R1 on the cleaning device within the airflow velocity simulation and emulation, as shown in Figure 6.

(a)   **(b)**
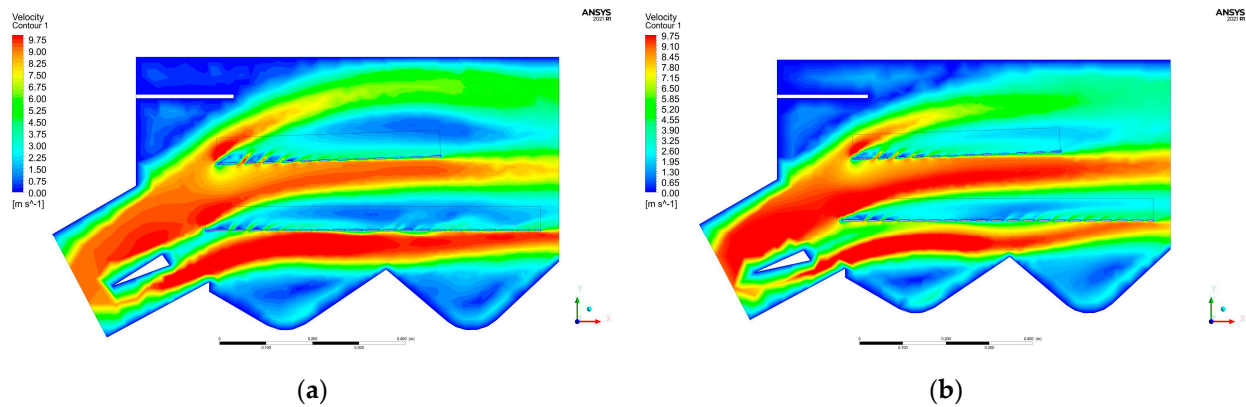
Figure 6. Variation of the velocity profile contour map of the inside of the cleaning chamber when the angle of the deflector plate is: (**a**) 32°; (**b**) 24°.

As can be seen from Figure 2, for the length direction of the cleaning chamber, the airflow speed tends to decrease from front to back; with the increase in the distance from the fan, the airflow generated by the fan cannot pass through the sieve holes at a wind speed suitable for cleaning at the rear part of the sieve surface, which is unfavorable to the cleaning operation. Given the same initial wind speed, the angle of the deflector plate has an effect on the wind speed distribution inside the cleaning chamber, and the deflector plate divides the airflow into the upper sieve airflow and the lower sieve airflow; the speed of the airflow is greater than that of the lower sieve in the upper sieve, and the airflow speed of the lower side of the two sieve surfaces is significantly greater than that of the upper side of the sieve surfaces; there exists an area of speed increase in the airflow field at the upper side of the front part of the deflector plate, and there exists a region of speed decrease in its rear part, and the upper sieve The high-speed airflow area formed in the front is conducive to making the dislodged material from the front vibrating deflector plate form a fluidized state in front of the sieve, which is convenient for the separation of impurities and grains. Different deflector angles have an influence on the wind speed of different sections and the magnitude of the impact.

Therefore, it is necessary to determine a reasonable angle of the deflector plate to effectively regulate the distribution of the airflow velocity in the cleaning chamber, so as to ensure that the airflow velocity in the main working area is favorable to the rapid separation of grains and impurities.

2.4. Bench Test of the Single Factor Test

According to the above analysis, the parameters affecting the scavenging loss rate of the combine harvester mainly include the thickness of the material layer and the airflow velocity. In order to verify the theoretical analysis made on the type of airflow field on the screen surface, the scavenging test was carried out on the scavenging test stand on the stripped wheat mixture.

The cleaning test bench is shown in Figure 7, which is mainly composed of a fan, a PLC controller, a deflector plate, an upper sieve assembly, a front and rear moving device for the wind speed sensor, a receiving box, a lower sieve assembly, upper and lower moving components for the wind speed sensor, a wind speed sensor, a feeding device, a motor, bearings, and an aluminum alloy frame. The upper sieve assembly and the lower sieve assembly are connected to the frame via ball head rods and fixed by bolt connections; the

wind speed sensor is installed on the connecting plate and fixed to the frame via the front and rear moving device as well as the upper and lower moving components. The fan, the feeding device, and the PLC controller are all connected to the frame by bolts. During the -operation of the test bench, the upper screen and the lower screen reciprocate in vibration, and threshing drum separation mixture enters the cleaning chamber through the feeding device. Under the action of gravity, it falls onto the upper screen surface and is continuously transported backward along the screen surface. Under the combined action of the sieve surface and the airflow, the clean grains fall through the two-layer sieve surface into the receiving box, and the debris is discharged from the rear to complete the entire cleaning process.
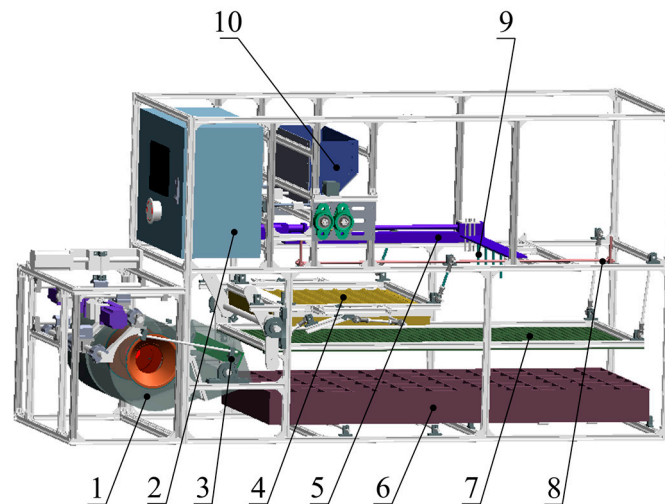
Figure 7. Structure of cleaning test bench. (1). Fan. (2). PLC controller. (3). Deflector plate. (4). Upper sieve assembly. (5). Front and rear moving device for the wind speed sensor. (6). Receiving box. (7). Lower sieve assembly. (8). Upper and lower moving components for the wind speed sensor. (9). Wind speed sensor. (10). Feeding device.

The test material was selected from Shandong Zibo Hefeng Seed Industry Science and Technology Co., Ltd. (Zibo, China), and the variety had a thousand grain weight of 336.4 g, an average moisture content of 17% in the kernel, and an average moisture content of 18.7% in the straw. In order to simulate the field harvesting conditions for the test, the grains, stalks, and other debris were mixed together in a certain proportion to simulate the detritus obtained in the actual harvesting process. The parameters of the working parts of the test were controlled by the operating console, which could change the fan speed by changing the current frequency, change the feeding amount of the stripped material by controlling the opening of the outlet of the bin and the speed of the feed rollers, and adjust the opening and closing angle of the wind diverter deflector plate by adjusting the wind diverter deflector plate adjuster. The impurity rate and loss rate of the grains were selected as the evaluation indexes of the test [26–28].

Before the test, the test bench will be emptied, idle running will be performed, and checks and debugging will be carried out. Once the operation of the test device is stable, the mixture will be poured into the hopper. Feeding of materials will begin under the joint action of the fan airflow and vibrating screen. Observe the screening process, and when all the screened material has been cleaned out, suspend the vibrating screen, fan, and feeding device. Collect all the materials in the receiving box under the sieve, manually clean out all the impurities, and then weigh and record the clean grains for calculation. To minimize the error and improve the accuracy of the test, each test was repeated three times, and finally, the average value was taken. The impurity rate and loss rate were calculated as follows:

The calculation formula of impurity rate is:

$$Y_1 = \frac{M_2}{M_1} \times 100\% \tag{14}$$

The calculation formula of loss rate is:

$$Y_2 = \frac{M_3}{M_1 + M_3} \times 100\% \tag{15}$$

where M_1 = clean grain quality under sieve, g; M_2 = quality of impurities under sieve, g; M_3 = cleaning outdoor grain quality.

2.5. Results of the Single Factor Test

In order to be able to select the factors that have a greater impact on the cleaning effect, and to determine the reasonable range of the level value in the orthogonal test, a single-factor test was carried out with the cleaning rate and loss rate of grains as the evaluation index of the performance advantages and disadvantages, and to seek for the influence of each factor on the cleaning performance of the cleaning device.

In this test, three of the above factors were selected to have a greater impact on the cleaning performance for experimental analysis, namely, feeding volume, fan deflector angle, fan speed, and seven levels were selected for each factor to obtain the influence of each factor on the impurity rate and loss rate. The table of experimental factor levels is shown in Table 1.

Table 1. Cleaning test factors and levels.

Level	Factors		
	Fan RPM A (r/min)	Angle of the Deflector Plate (°)	Feed Rate (kg/s)
1	750	16	8.0
2	800	20	8.8
3	850	24	9.6
4	900	28	10.4
5	950	32	11.2
6	1000	36	12
7	1050	40	12.8

Sequentially adjust the level of variable factors to other levels. Each test in addition to the variable factors of the other two factors employed commonly used work parameters as a fixed value for the 0 level. Repeat the previous operation, respectively, the three test factors for the clearing test, to explore the relationship between the factors and the test evaluation indexes.

2.6. Bench Test of Orthogonal Test

In order to further analyze the influence of various factors on the cleaning performance and determine whether there is an interaction between the factors, a better level was selected for orthogonal testing based on the range of single factor tests. The fan speed (A), Feed rate (B), and Angle of the deflector plate (C) were selected as the experimental factors, and the corn impurity rate (Y1) and corn loss rate (Y2) were used as the evaluation indexes, as shown in Table 2. The experiment consisted of 17 treatments, and each treatment was repeated to take the average value.

**Table 2.** Orthogonal test factor level control table.

Level	Factors		
	Fan RPM A (r/min)	**Feed Rate B (kg/s)**	**Angle of the Deflector Plate C (°)**
1	850	8.8	20
2	900	9.6	24
3	950	10.4	28

3. Results

3.1. Bench Test

3.1.1. Single-Factor Test of the Angle of the Deflector Plate

Keeping the feed rate at 10 kg/s, the opening of the upper sieve fish scale sieve at 247°, the sieve size of the lower sieve round hole sieve at 8 mm, and the fan speed at 900 r/min unchanged, seven levels were selected in the angle of the deflector plate between 16–40°, and the levels of the variables were adjusted to the other levels in turn and tests were carried out, and the tests in each set of tests were repeated for three times, and the average value of each test was recorded. The variation of cleaning effect with the angle of the deflector plate is shown in Figure 8.
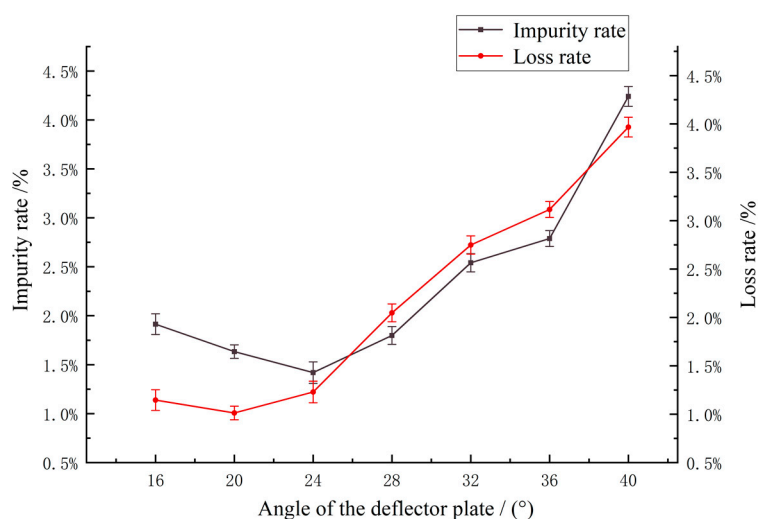

Figure 8. Influence of angle of the deflector plate on cleaning performance.

As can be seen from Figure 7, the impurity rate of grains showed a trend of decreasing and then increasing with the increase in the deflector angle, and the impurity rate decreased in the range of angle of the deflector plate from 16° to 32°, and increased significantly with the increase in rotational speed after 32°. The seed loss rate fluctuated less in the range of turning angles from 16° to 32°, and the loss rate began to increase continuously after 32°.

The influence of angle of the deflector plate on the impurity rate is more complicated Lower or higher rotational turning angles will affect the impurity rate. A lower deflector speed means that the impurities can not be effectively excluded at one time. With the increase in the deflector angle, the grain through the sieve will increase, but the entrained discharged grain will also increase, resulting in a rise in the impurity rate; the loss rate shows a trend of increasing with the increase in the deflector. At 24°, the impurity rate and loss rate are lower, and the cleaning effect is the best. For comprehensive consideration, it is more suitable to take the angle of the deflector plate as 20°, 24°, and 28° in the orthogonal test.

3.1.2. Single Factor Test of Fan Speed

Keeping the feeding rate of 10 kg/s, the opening of the upper sieve fish scale sieve is 24°, the sieve size of the lower sieve round hole sieve is 8 mm, and the angle range of the guide plate is 28°, the fan speed range is 750~1050 r/min. Seven levels were selected to adjust the variable factor level to other levels and test. The cleaning effect changes with the fan speed are shown in Figure 9.
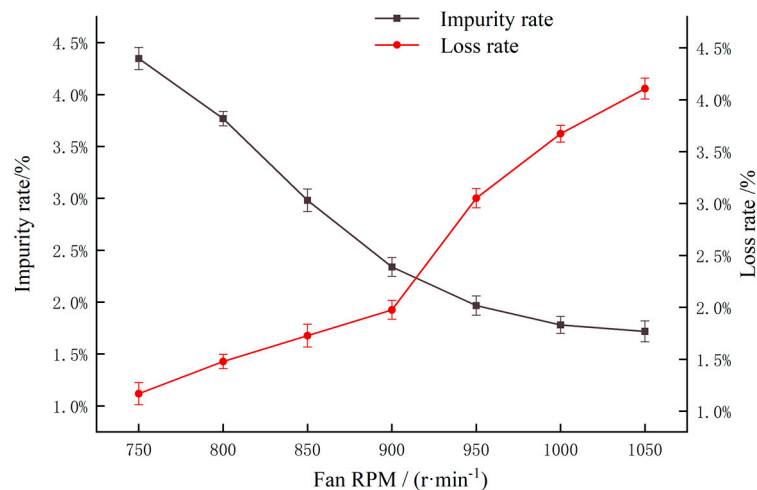
Figure 9. Influence of Fan RPM on cleaning performance.

The speed of the fan is the main factor affecting the cleaning effect. It can be seen from Figure 2 that the impurity rate of the grains decreases gradually with the increase in the rotation speed of the fan. The impurity rate of the grains remains basically unchanged when the rotation speed of the fan is in the range of 900~1050 r/min, and the loss rate of the grains increases with the increase in the rotation speed of the fan. The reason may be that as the wind speed exceeds the suspension speed of the grains, the grains are not sieved and are directly blown out of the cleaning room, resulting in a gradual decrease in the impurity rate and an increase in the loss rate. At about 920 r/min, the impurity rate and loss rate are low, and the cleaning effect is the best. Considering comprehensively, it is more appropriate to take the fan speed of 850, 900, and 950 r/min in the orthogonal test.

3.1.3. Single Factor Test of Feeding Rate

We kept the opening of the upper sieve fish-scale sieve at 24°, the size of the sieve hole of the lower sieve round-hole sieve at 8 mm, the angle range of the deflector at 36°, and the working condition of the fan speed at 950 r/min unchanged. Seven levels were selected between the feeding range of 8–12.8 kg/s, and the variable factor levels were adjusted to other levels in turn and tested. The cleaning quality changes with the feeding rate as shown in Figure 9.

It can be seen from Figure 10 that the impurity rate of grains decreased slowly and then increased with the increase in feeding rate. The impurity rate and loss rate decreased slowly in the range of 8~9.6 kg/s. After 9.6 kg/s, the impurity rate increased with the increase in feeding rate. The loss rate began to rise after 9.6 kg/s, and the loss rate rose sharply after 12 kg/s.

This is because when the feeding rate is small, the resistance of the material to the airflow is small, and the airflow velocity and wind pressure are large. The material to be cleaned is easily blown out of the cleaning room, and the loss of grain cleaning is large. With the increase in feeding rate, the accumulation on the sieve surface becomes thicker, and the material cannot be effectively cleaned. The stems and grains are not screened out of the discharge port in a timely way, so the loss rate becomes larger. In addition, as the feeding rate continued to increase, the number of stems through the sieve increased, so the

impurity rate showed an increasing trend. At 9.6 kg/s, the impurity rate and loss rate are low, and the cleaning effect is the best. All things considered, the orthogonal test feeding rate of 8.8, 9.6, 10.4 kg/s is more appropriate.
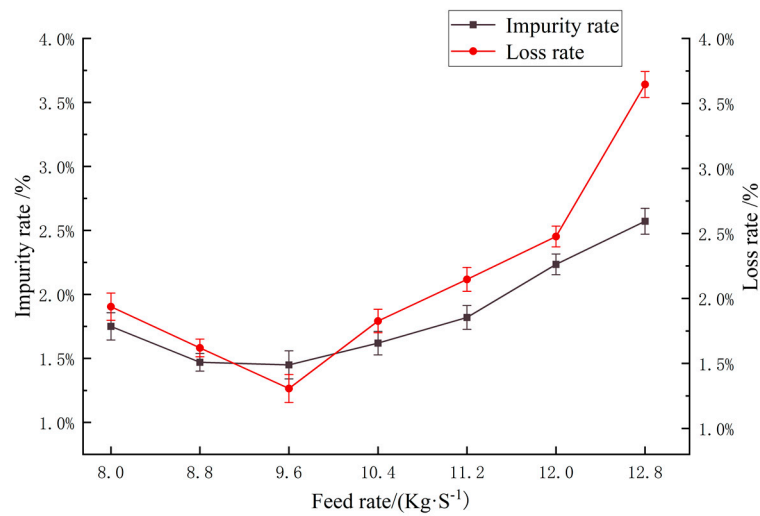

Figure 10. Influence of feed rate on cleaning performance.

3.2. Results of the Orthogonal Test and Variance Analysis

The test results are shown in Table 3. The test results were analyzed by variance analysis, loss of fit test, and regression fitting.

Table 3. Orthogonal test results.

Test No.	Fan RPM A/(r/min)	Feed Rate B/(kg/s)	Angle of the Deflector Plate C/(°)	Loss Rate Y1/(%)	Y2/(%)
1	950	9.6	20	1	4.51
2	950	10.4	24	0.69	4.39
3	950	8.8	24	1.28	4.22
4	900	9.6	24	1.11	2.55
5	900	9.6	24	1.51	2.58
6	900	9.6	24	1.34	2.68
7	850	10.4	24	3.14	3.51
8	850	8.8	24	4.45	2.86
9	900	10.4	20	1.28	3.57
10	850	9.6	28	4.43	3.02
11	900	8.8	28	2.73	2.98
12	900	9.6	24	1.09	2.72
13	850	9.6	20	3.2	3.15
14	900	8.8	20	2.4	3.16
15	950	9.6	28	1.29	4.03
16	900	10.4	28	2.59	3.25
17	900	9.6	24	1.28	2.64

The results are shown in Table 4. For grains loss rate $Y1$, the model effect was significant ($p < 0.01$), indicating that the model was effective. The model determination coefficient R2 reaches 0.9919, and the model correction coefficient r2adj = 0.9816 indicates that the model fitting accuracy is high and the model is reliable. The p value of the loss of fit test is 0.6018, indicating that the loss of fit is not significant, the error is small, and the center fitting is good. The test factors are fan speed A, feeding rate B, angle of the deflector plate

C. Square terms A^2, B^2, and C^2 are extremely significant; the effect of cross terms AC, BC, is significant; the obtained regression equation is:

$$Y1 = 1.27 - 1.37A - 0.395B + 0.395C - 0.235AC + 0.245BC \\ +0.677A^2 + 0.477B^2 + 0.537C^2$$

(16)

Table 4. Analysis of Variance for impurity rate.

Source	Sum of Squares	Degree of Freedom	Mean Square	F-Value	*p*-Value	Significant Level
Model	22.54	9	2.50	95.62	0.0000017	significant
A	15.02	1	15.02	573.35	0.0000001	**
B	1.25	1	1.25	47.66	0.0002305	**
C	1.25	1	1.25	47.66	0.0002305	**
AB	0.1296	1	0.1296	4.95	0.0614611	
AC	0.2209	1	0.2209	8.43	0.0228453	*
BC	0.2401	1	0.2401	9.17	0.0191716	*
A2	1.9298	1	1.9298	73.69	0.0000580	**
B2	0.8413	1	0.8413	32.12	0.0007602	**
C2	1.2142	1	1.2142	46.36	0.0002511	**
Residual	0.1833	7	0.0262			
Lack of Fit	0.0628	3	0.0209	0.6948	0.6017686	not significant
Pure Error	0.1205	4	0.0301			
Cor Total	22.72	16				
R^2	0.9919					
Adjusted R^2	0.9816					

Note: ** means $p \leq 0.01$ (very significant), * means $p \leq 0.05$ (more significant).

The results are shown in Table 5. For the impurity rate $Y2$, the model effect was significant ($p < 0.01$), indicating that the model was effective; the model determination coefficient R2 reaches 0.9962, and the model correction coefficient r2adj = 0.9914 indicates that the model fitting accuracy is high and the model is reliable. The p value of the loss of fit test is 0.7521, indicating that the loss of fit is not significant, the error is small, and the center fitting is good. The test factors are fan speed A, feeding rate B, angle of the deflector plate C, cross term AB, square terms A^2, B^2, and C^2. The effect of the cross-term AC is significant; the obtained regression equation is:

$$Y2 = 2.63 + 0.5763A + 0.1875B - 0.1387C - 0.12AB - 0.0875AC \\ +0.7742A^2 + 0.3368^20.2692C^2$$

(17)

Table 5. Analysis of Variance for loss rate.

| Source	Sum of Squares	Degree of Freedom	Mean Square	F-Value	*p*-Value	Significant Level
Model	6.77	9	0.7527	205.87	0.0000001	significant
A	2.66	1	2.6565	726.53	0.0000001	**
B	0.28	1	0.2813	76.92	0.0000505	**
C	0.15	1	0.1540	42.12	0.0003373	**
AB	0.0576	1	0.0576	15.75	0.0053991	**
AC	0.0306	1	0.0306	8.38	0.0231811	*
BC	0.0049	1	0.0049	1.34	0.2849842	
A^2	2.5241	1	2.5241	690.31	0.0000001	**
B^2	0.4775	1	0.4775	130.59	0.0000088	**
C^2	0.3052	1	0.3052	83.48	0.0000387	**
Residual	0.0256	7	0.0037			
Lack of Fit	0.0061	3	0.0020	0.4150	0.7520831	not significant
Pure Error	0.0195	4	0.0049			
Cor Total	6.80	16				
R^2	0.9962					
Adjusted R^2	0.9914					

Note: ** means $p \leq 0.01$ (very significant), * means $p \leq 0.05$ (more significant).

The results of orthogonal tests show that according to the regression coefficient of each factor in the regression model, the significant order of the influence of each factor on the impurity rate and loss rate is consistent, and the order of influence from large to small is fan speed, angle of the deflector plate, and feed rate.

In order to clearly observe the interaction between factors for the relationship between impurity rate and loss rate, response surface plots were drawn by Design-Expert 13.0.1.0 64-bit and the results were analyzed.

Figure 11a shows the response surface plot of fan speed versus feed rate, where the loss rate reaches its maximum at a high level of both fan speed and feed rate. For a given fan speed, the loss rate first decreases slightly with higher feed rate and then increases. At a certain feed rate, the loss rate decreases slowly and then increases rapidly as the fan speed increases. From the trend of the curves in the figure, it can be seen that the effect of fan speed on the loss rate is more significant than that of the feed rate. The interaction effect was analyzed as follows: a higher fan speed and a larger feeding amount shortened the cleaning time of the discharged material, which resulted in the rapid discharge of the grains, reduced the chance of the grains passing through the sieve, and led to the increase in the loss rate.
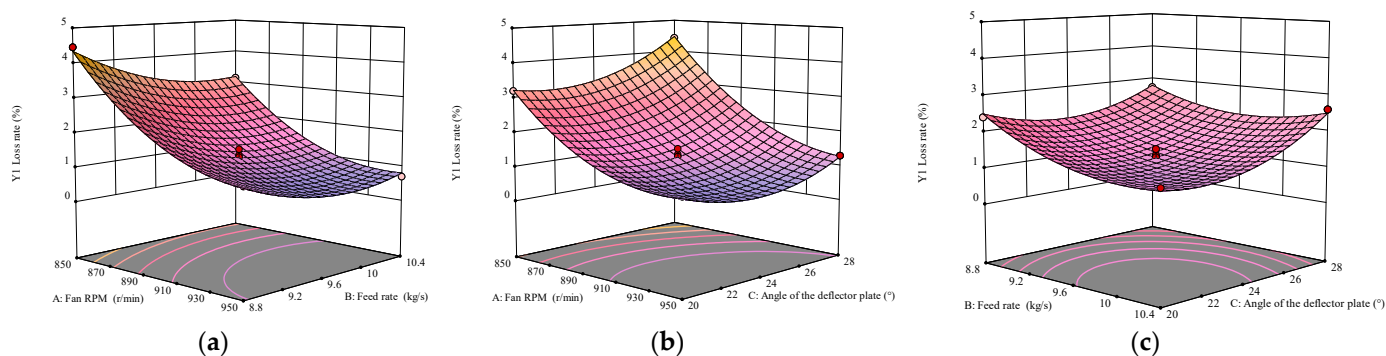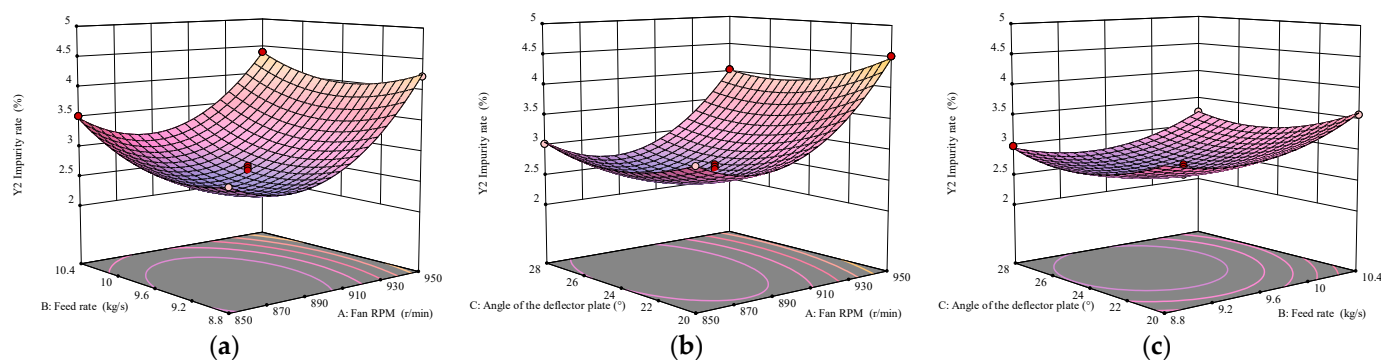

Figure 11. Effects of the interaction of factors on the loss rate. (**a**) Effect of the fan speed and feed rate on the loss rate. (**b**) Effect of the fan speed and angle of the deflector plate on the loss rate. (**c**) Effect of the feed rate and angle of the deflector plate on the loss rate.

Figure 11b shows the response surface of fan speed and deflector angle. The loss rate reaches its maximum value when the fan speed is at a high level and the deflector angle is at a low level. When the fan speed is fixed and the deflector angle increases, the loss rate decreases slowly and then rises slightly. When the deflector angle is fixed, with the increase in fan speed, the loss rate decreases slowly and then increases rapidly. From the trend of the curves in the figure, it can be seen that the fan speed has a more significant effect on the loss ratio than the deflector angle. The interaction effect was analyzed as the smaller deflector angle directed the high-speed airflow to the middle and back of the screen surface, resulting in clean grains being blown out directly by the fan, and increasing the difficulty of the grains to pass through the screen, leading to a higher loss rate.

Figure 11c shows the response surface of the feed rate and the deflector angle. The loss rate reaches the maximum value when the feed rate and the deflector angle are both at a low level. At a given feed rate, as the deflector angle increases, the loss rate decreases slowly and then increases slowly. When the angle of the deflector is fixed, the loss rate decreases first and then increases slowly with the increase in the feeding volume. The curve trend can be seen from the figure. The influence of the feeding amount and the deflector angle on the loss rate of the small change the interaction between the deflector angle and the smaller feeding amount leads to the screen surface tail air velocity rising, resulting in the clean grains being directly blown out by the fan out of the tail of the screen surface of, and the loss rate increases.

Figure 12a shows the response surface plot of fan speed versus feed rate, from which it can be seen that the impurity rate reaches its maximum value when both fan speed and

feed rate are at a low level. When the fan speed is fixed, with an increase in the feeding amount, the impurity rate decreases slowly, and then the change is not obvious at a high level. When the feeding amount is fixed, the higher the fan speed, the lower the impurity rate. From the trend of the curve on the graph, it can be seen that the effect of fan speed on the impurity rate is more significant than the crank speed.

Figure 12. Effects of the interaction of factors on the loss rate. (**a**) Effect of the fan speed and feed rate on the impurity rate. (**b**) Effect of the fan speed and angle of the deflector plate on the impurity rate. (**c**) Effect of the feed rate and angle of the deflector plate on the impurity rate.

I confirm Figure 12b shows the response surface of fan speed and deflector angle. The impurity rate reaches the maximum value when the fan speed is at a low level and the deflector angle is at a high level. When the fan speed is fixed, as the deflector angle is larger, the impurity rate first decreases and then tends to be unchanged. When the deflector angle is fixed, with the increase in fan speed, the impurity rate shows a decreasing trend. From the trend of the curve on the graph, it can be seen that the effect of fan speed on the impurity rate is obviously more significant than the angle of the deflector.

The interaction effect is analyzed as follows: a low fan speed leads to larger deflector angle which directs the airflow to the front of the screen, so that the screening capacity of the cleaning device for the light impurities in the middle and back of the screen surface is weakened, increasing the chances of impurity penetration of the screen, resulting in an increased impurity rate increased.

Figure 12c shows the response surface of the feed rate and the deflector angle, and the impurity rate reaches the maximum value when the deflector angle is at a high level and the feeding volume is at a low level. When the feed rate is fixed, the larger the deflector angle is, the higher the impurity rate is. When the deflector angle is fixed, the larger the feeding amount, the lower the impurity rate. From the trend of the curve in the figure, it can be seen that the effect of the deflector angle on the impurity rate is more significant than the feed rate.

The analysis of the interaction effect is that a lower feed rate and higher deflector angle make the airflow velocity at the front of the screen too large, resulting in a larger loss of seed cleaning, and the airflow velocity at the back of the screen is small, which increases the chances of the impurity penetrating the screen, resulting in the increase in the impurity rate.

3.3. Results of the Parameter Optimization and Verification Test

Taking the fan speed, feeding volume, and deflector angle as optimization variables, and taking the minimum seed impurity rate and seed loss rate as optimization indexes, multi-objective parameter optimization was carried out to solve the optimal parameter combinations. The optimal parameter combinations for the cleaning effect were fan speed 903.57 r/min, feeding volume 7.49 kg/s, and deflector angle 23.77°; at this time, the obtained seed impurity rate was 1.14%, and the seed loss rate was 2.69%. The optimal parameters were rounded to verify the test, and the fan speed was set at 900 r/min, the

feeding volume was 7.5 kg/s, and the angle of the deflector plate was 24°. The test steps were the same as those described before, and five repetitions were carried out to find the average value, which resulted in a loss rate of 1.27% and an impurity rate of 2.41%. The results of the validation test and the optimized regression prediction were relatively small, and the model of the regression equation was more reliable.

4. Conclusions

1. Taking the corn and material layer as the research object, force analysis and motion analysis of the material on the sieve subject to air flow were carried out, and it was deduced that the pressure drop across the sieve was related to the porosity, the thickness of the material layer, and the density of the material on the sieve, and affected its fluidization state. When the pressure drop across the sieve is too large, more than the dynamic pressure provided by the cleaning device, it will lead to the transformation of the sieve fluidization state to the static state, increasing the impurity rate of the grain; on the contrary, if the pressure drop across the sieve is too small it will lead to the sieve fluidization in the "boiling" state, increasing the cleaning loss. For a given grain combine harvester, with the change of feeding, there is a need to adjust the airflow rate to meet the sieve reasonable fluidization needs;

2. The law of the scavenging airflow field was analyzed, and single-factor tests were carried out on the rotational speed of the deflector angle, the rotational speed of the blower, and the feeding amount, and the law whereby the scavenging performance changes with each factor was derived. Screening efficiency and loss rate were selected as test indexes, and a three-factor three-level orthogonal test with response surface analysis was conducted. The test results show that the interaction of fan speed and deflector angle has a significant effect on the impurity rate and loss rate. Analyzing the interaction of the factors, the significance order of the effects of the factors on the impurity rate and loss rate was the same, and the order of the effects was, from the largest to the smallest, the fan speed, the angle of the deflector plate, and the feeding amount;

3. The experimental regression equation model was established according to the test results, and the optimal working condition combination of the work was found to be a fan speed of 900 r/min, a feeding volume of 7.5 kg/s, and a 24° angle of the deflector plate. According to the rounded and more optimal working parameters, several verification tests were carried out, and the impurity rate and the loss rate were 1.27% and 2.41%, respectively. The results of the validation tests coincide with the optimized regression predictions, and the optimized parameters are reliable.

Author Contributions: Conceptualization, D.L. and D.G.; methodology, D.L. and Z.Z.; software, D.L.; validation, D.L., D.G., and D.Y.; formal analysis, D.L.; investigation, D.L.; resources, Q.H.; data curation, D.L.; writing—original draft preparation, D.L.; writing—review and editing, D.G.; visualization, J.Y., P.G., and Q.H.; supervision, D.G.; project administration, D.G.; funding acquisition, D.G. All authors have read and agreed to the published version of the manuscript.

Institutional Review Board Statement: Not applicable.

Data Availability Statement: Data are contained within the article.

Conflicts of Interest: The authors declare no conflicts of interest.

References

1. Su, T.S.; Han, Z.D.; Cui, J.W.; Wang, G.X.; Hao, X.M.; Hao, F.P.; Han, K.L. Research Status and Development Trend of Cleaning Unit of Cereal Combine Harvesters. *J. Agric. Mech. Res.* **2016**, *38*, 6–11.

2. Liu, P.; Jin, C.; Yang, T.; Chen, M.; Ni, Y.; Yi, X. Design and Experiment of Multi Parameter Adjustable and Measurable Cleaning System. *Trans. Chin. Soc. Agric. Mach.* **2020**, *51*, 191–201.

3. Liang, Z.; Wada, M.E. Development of cleaning systems for combine harvesters: A review. *Biosyst. Eng.* **2023**, *236*, 79–102. [CrossRef]

4. Chuan-Udom, S.; Chinsuwan, W. Operating factors affecting harvesting losses of cleaning unit of rice combine harvesters. *Asia-Pac. J. Sci. Technol.* **2017**, *15*, 487–495.

5. Yang, L.; Lizhang, X.; Ying, Z.; Baijun, L.; Zhenwei, L.; Yaoming, L. Effects of throughput and operating parameters on cleaning performance in air-and-screen cleaning unit: A computational and experimental study. *Comput. Electron. Agric.* **2018**, *152*, 141–148.

6. Chai, X.; Zhou, Y.; Xu, L.; Li, Y.; Li, Y.; Lv, L. Effect of guide strips on the distribution of threshed outputs and cleaning losses for a tangential-longitudinal flow rice combine harvester. *Biosyst. Eng.* **2020**, *198*, 223–234. [CrossRef]

7. Li, H.; Li, Y.; Gao, F.; Zhao, Z.; Xu, L. CFD–DEM simulation of material motion in air-and-screen cleaning device. *Comput. Electron. Agric.* **2012**, *88*, 111–119. [CrossRef]

8. Dai, F.; Song, X.; Shi, R.; Zhao, W.; Guo, W.; Zhang, Y. Migration law of flax threshing materials in double channel air-and-screen separating cleaner. *Int. J. Agric. Biol. Eng.* **2021**, *14*, 81–90. [CrossRef]

9. Li, X.; Zhang, J.; Ji, J. Analysis of Airflow Velocity Field Characteristics of an Oat Cleaner Based on Particle Image Velocimetry Technology. *Appl. Eng. Agric.* **2019**, *35*, 193–201. [CrossRef]

10. Zhang, C.; Geng, D.; Xu, H.; Li, X.; Ming, J.; Li, D.; Wang, Q. Experimental Study on the Influence of Working Parameters of Centrifugal Fan on Airflow Field in Cleaning Room. *Agriculture* **2023**, *13*, 1368. [CrossRef]

11. Liang, Z.; Xu, L.; De Baerdemaeker, J.; Li, Y.; Saeys, W. Optimisation of a multi-duct cleaning device for rice combine harvesters utilising CFD and experiments. *Biosyst. Eng.* **2020**, *190*, 25–40. [CrossRef]

12. Liang, Z.; Li, Y.; Xu, L. Grain Sieve Loss Fuzzy Control System in Rice Combine Harvesters. *Appl. Sci.* **2019**, *9*, 114. [CrossRef]

13. Hou, J.; Liu, X.; Zhu, H.; Ma, Z.; Tang, Z.; Yu, Y.; Jin, J.; Wang, W. Design and Motion Process of Air-Sieve Castor Cleaning Device Based on Discrete Element Method. *Agriculture* **2023**, *13*, 1130. [CrossRef]

14. Ma, Z.; Han, M.; Li, Y.; Gao, H.; Ma, K. Motion of cereal particles on variable-amplitude sieve as determined by high-speed image analysis. *Comput. Electron. Agric.* **2020**, *174*, 105465. [CrossRef]

15. Liang, Y.; Tang, Z.; Zhang, H.; Li, Y.; Ding, Z.; Su, Z. Cross-flow fan on multi-dimensional airflow field of air screen cleaning system for rice grain. *Int. J. Agric. Biol. Eng.* **2022**, *15*, 223–235. [CrossRef]

16. Tang, Z.; Li, Y.; Li, h.; Xu, l.; Zhao, Z. Analysis on the Eddy Current of the Air-and-screen Cleaning Device. *Trans. Chin. Soc. Agric. Mach.* **2010**, *41*, 62–66.

17. Ahuja, M.; Dogra, B.; Narang, M.; Dogra, R. Development and Evaluation of Axial Flow Paddy Thresher Equipped with Feeder Chain Type Mechanical Feeding System. *Curr. J. Appl. Sci. Technol.* **2017**, *23*, 1–10. [CrossRef]

18. Fu, X.; Yao, Z.; Zhang, X. Numerical simulation of polygonal particles moving in incompressible viscous fluids. *Particuology* **2017**, *31*, 140–151. [CrossRef]

19. Wee Chuan Lim, E.; Wang, C.-H.; Yu, A.-B. Discrete element simulation for pneumatic conveying of granular material. *AIChE J.* **2006**, *52*, 496–509. [CrossRef]

20. Ren, B.; Zhong, W.; Chen, Y.; Chen, X.; Jin, B.; Yuan, Z.; Lu, Y. CFD-DEM simulation of spouting of corn-shaped particles. *Particuology* **2012**, *10*, 562–572. [CrossRef]

21. El-Emam, M.A.; Zhou, L.; Shi, W.; Han, C.; Bai, L.; Agarwal, R. Theories and Applications of CFD–DEM Coupling Approach for Granular Flow: A Review. *Arch. Comput. Methods Eng.* **2021**, *28*, 4979–5020. [CrossRef]

22. Tavoularis, S.; Nedić, J. *Measurement in Fluid Mechanics*; Cambridge University Press: Cambridge, UK, 2024.

23. Xia, L.L.; Jin, Y.L.; Li, Y.M.; Tang, Z.F. Experimental Study of Air Flow Field of Air-and-screen Cleaning. *J. Agric. Mech. Res.* **2009**, *31*, 188–190+196.

24. Li, Y.; Tang, Z.; Li, H.; Zhao, Z.; Xu, L. Experiment on the flow field of the air-and-screen cleaning device. *Trans. Chin. Soc. Agric. Mach.* **2009**, *40*, 80–83.

25. Badretdinov, I.; Mudarisov, S.; Lukmanov, R.; Permyakov, V.; Ibragimov, R.; Nasyrov, R. Mathematical modeling and research of the work of the grain combine harvester cleaning system. *Comput. Electron. Agric.* **2019**, *165*, 104966. [CrossRef]

26. Chenlong, F.; Tao, C.; Dongxing, Z.; Li, Y.; Congcong, T.; Xiangjun, Z.; University, C.A. Design and Experiment of Double-layered Reverse Cleaning Device for Axial Flow Combine Harvester. *Trans. Chin. Soc. Agric. Mach.* **2018**, *49*, 239–248.

27. Liang, Z.; Li, Y.; Baerdemaeker, J.D.; Xu, L.; Saeys, W. Development and testing of a multi-duct cleaning device for tangential-longitudinal flow rice combine harvesters. *Biosyst. Eng.* **2019**, *182*, 95–106. [CrossRef]

28. Korn, C. Numerical and Experimental Tests of Separation in a Combine Cleaning Device. In *Application of Coupled CFD-DEM Simulation to Separation Process in Combine Harvester Cleaning Devices*; Korn, C., Ed.; Springer: Berlin/Heidelberg, Germany, 2020; pp. 108–169.